Article

Discovery Medicine 2025; 37(203): 3051–3063
https://doi.org/10.24976/Discov.Med.202537203.255

Impact of Aberrant CLDN18.2 Expression on Intercellular Junction Stability in Gastric Cancer Cells

Wenxi Li[1], Mingkai Chen[2], Biao Qian[3], Xiao Li[4,*]

[1]Department of Surgery, Xuzhou Hejia Hospital, 221004 Xuzhou, Jiangsu, China
[2]Department of Gastroenterology, Zhengzhou Yihe Hospital, 450000 Zhengzhou, Henan, China
[3]Intensive Care Unit, Xuzhou Hejia Hospital, 221004 Xuzhou, Jiangsu, China
[4]Internal Medicine Department, Xuzhou Hejia Hospital, 221004 Xuzhou, Jiangsu, China
*Correspondence: xiaozaixinyi@163.com (Xiao Li)
Submitted: 29 October 2025 Revised: 24 November 2025 Accepted: 1 December 2025 Published: 20 December 2025

Background: Disruption of epithelial tight junctions (TJs) promotes loss of polarity and increased invasiveness in gastric cancer. Claudin-18.2 (CLDN18.2), a stomach-specific TJ protein, is frequently downregulated or mislocalized in tumors. However, its functional role remains unclear. This study investigated how CLDN18.2 regulates tight junction integrity and interacts with junction-associated proteins in gastric cancer cells.

Methods: CLDN18.2 expression and subcellular localization in gastric cancer cells (MKN45) and normal gastric epithelial cells (GES-1) were examined using Western blotting and immunofluorescence. CLDN18.2 was silenced using siRNA in MKN45 and SNU-16 cells, and epithelial barrier function was evaluated by transepithelial electrical resistance (TEER) and fluorescein isothiocyanate (FITC)-Dextran permeability assays. The effects of CLDN18.2 knockdown on tight junction and adherens junction proteins were analyzed by Western blotting. Cell migration and invasion were evaluated using Transwell assays and wound-healing assays in MKN45 cells. Co-immunoprecipitation (Co-IP) was performed to validate CLDN18.2–Zonula occludens-1 (ZO-1) interactions, and rescue experiments with ZO-1 overexpression were performed to determine its ability to restore tight junction integrity following CLDN18.2 silencing. An orthotopic gastric cancer xenograft model was established in BALB/c nude mice using stably transfected MKN45 cells.

Results: CLDN18.2 was highly expressed in MKN45 cells and predominantly localized at the plasma membrane, co-localizing with ZO-1 and occludin. CLDN18.2 knockdown significantly reduced ZO-1, occludin, E-cadherin, and β-catenin expression ($p < 0.001$), decreased TEER, and increased FITC-Dextran permeability ($p < 0.001$), while markedly enhancing cell migration and invasion ($p < 0.01$). Pull-down assays confirmed that CLDN18.2 forms a complex with ZO-1 in an expression-dependent manner. ZO-1 overexpression partially restored tight junction protein levels and barrier function impaired by CLDN18.2 knockdown. *In vivo*, silencing of CLDN18.2 significantly increased the number of metastatic nodules in the orthotopic xenograft model ($p < 0.001$). In contrast, overexpression of ZO-1 effectively reversed this pro-metastatic effect and restored junctional protein expression.

Conclusion: CLDN18.2 maintains tight junction integrity in gastric cancer cells through interaction with ZO-1. Its downregulation disrupts cell-cell junctions, weakens epithelial barrier function, and promotes cell migration and invasion, whereas compensatory ZO-1 overexpression can partially reverse these effects. These findings reveal a key regulatory role of CLDN18.2 in gastric cancer progression, offering mechanistic support for CLDN18.2-targeted therapeutic strategies.

Keywords: gastric cancer; Claudin-18.2; ZO-1; tight junction; epithelial barrier function

Introduction

Gastric cancer is among the five most prevalent and lethal malignancies worldwide, with a particularly high burden in Asian populations [1,2]. Most patients are diagnosed at advanced stages, and the 5-year survival rate remains approximately 6% [3,4]. A pivotal driver of gastric carcinogenesis and progression is the compromise of the epithelial barrier. In particular, dismantling of tight junction (TJ) complexes is a hallmark event that triggers loss of epithelial polarity, attenuation of intercellular adhesion, and increased motility and invasiveness, processes closely associated with epithelial–mesenchymal transition (EMT) [5]. Despite these insights, the precise molecular pathways that orchestrate TJ disruption in gastric cancer, as well as their ensuing impact on invasion and metastasis, remain only partially defined.

The Claudin family comprises transmembrane proteins that are essential for the assembly and maintenance of tight junctions. Claudin 18.2 (CLDN18.2), a stomach-specific isoform of Claudin 18, is predominantly localized at tight junctions within normal gastric epithelium, where it

preserves epithelial polarity and reinforces barrier integrity [6,7]. In gastric cancer, CLDN18.2 expression is frequently reduced or mislocalized, including loss from the plasma membrane and aberrant accumulation in the cytoplasm or nucleus [8]. Previous studies reported substantial interpopulation differences in CLDN18.2 expression, with ~17% of German patients showing high expression in primary tumors [9]. In a Japanese cohort, CLDN18.2 was detected in 87% of primary tumors and 80% of lymph node metastases, with high expression observed in 52% of primary tumors and 45% of lymph node metastases [10]. Clinically, low CLDN18.2 expression is correlated with an increased risk of peritoneal metastasis, whereas higher expression is associated with an elevated risk of bone metastasis [11]. These findings suggest that CLDN18.2 plays a pivotal role in maintaining intercellular junctional stability and represents a promising target for therapeutic intervention. Nevertheless, the detailed mechanisms through which CLDN18.2 regulates tight junction integrity and coordinates with other junctional components remain incompletely characterized.

Within the TJ complex, ZO-1 (Zonula occludens-1) serves as a scaffold protein, anchoring membrane proteins such as occludin and Claudins to the actin cytoskeleton and thereby maintaining structural continuity and functional stability [12]. Occludin is essential for epithelial barrier function, and its loss increases paracellular permeability and promotes cell migration [13]. Moreover, E-cadherin, a core adherens junction protein, plays a pivotal role in EMT by facilitating the transition of epithelial tumor cells toward a mesenchymal phenotype and enhancing their invasive and metastatic potential [14–16]. Building on these observations, we hypothesize that CLDN18.2 contributes to the stabilization of tight junctions and the maintenance of epithelial barrier integrity by forming a complex with ZO-1, whereas its suppression disrupts junctional architecture and facilitates tumor cell motility and invasion.

In the present study, we aimed to elucidate the subcellular localization and functional role of CLDN18.2 within gastric cancer cell tight junctions. We evaluated the consequences of CLDN18.2 downregulation on barrier properties, junctional protein expression, and invasive behavior, and confirmed its interaction with ZO-1 through co-immunoprecipitation and rescue assays. Collectively, our results clarify the mechanistic contribution of CLDN18.2 to gastric cancer progression and provide a rationale for the development of therapeutic strategies targeting tight junctions.

Materials and Methods

Cell Lines and Culture

Human gastric carcinoma cell lines MKN45 and SNU16, along with the normal gastric epithelial cell line GES1, were obtained from the Cell Bank of the Chinese Academy of Sciences (Shanghai, China). Cells were maintained in Roswell Park Memorial Institute (RPMI)1640 medium (L211013, Basalmedia Biotechnology, Shanghai, China) supplemented with 10% fetal bovine serum (PSFB5SA, Peak Inc., Los Angeles, CA, USA) and 1% penicillin-streptomycin (15140122, Thermo Fisher Scientific, Waltham, MA, USA) under standard culture conditions at 37 °C in a humidified incubator with 5% CO_2. Subculture was performed when cells reached 70–80% confluence using 0.25% trypsin-Ethylenediaminetetraacetic Acid (EDTA) (S310KJ, Beyotime Biotechnology, Shanghai, China). All cell lines were authenticated by short tandem repeat (STR) profiling and routinely screened for mycoplasma contamination, with negative results confirmed prior to experimental use.

Quantitative Real-Time PCR (qPCR)

Total RNA was extracted using TRIzol™ reagent (15596026, Thermo Fisher Scientific, Waltham, MA, USA), and cDNA was synthesized with the Goldenstar™ RT6 cDNA Synthesis Kit Ver.2 (TSK302M, Tsingke Biotechnology, Beijing, China). qPCR reactions were performed using 2× T5 Fast qPCR Mix (SYBR Green I) (TSE002, Tsingke Biotechnology, Beijing, China) on a Real-Time PCR Detection System (IQ5, Bio-Rad, Hercules, CA, USA). The amplification protocol consisted of 95 °C for 30 s, followed by 40 cycles at 95 °C for 5 s and 60 °C for 30 s. Relative gene expression was calculated using the $2^{-\Delta\Delta Ct}$ method, with Glyceraldehyde-3-Phosphate Dehydrogenase (GAPDH) as the internal control.

Primer sequences were as follows:

CLDN18.2-F: 5′-TGTGCGCCACCATGGCCGTG-3′;

CLDN18.2-R: 5′-GTGCTGAGAGGTCTTAGAGC-3′;

ZO-1-F: 5′-GTCCAGAATCTCGGAAAAGTGCC-3′;

ZO-1-R: 5′-CTTTCAGCGCACCATACCAACC-3′;

GAPDH-F: 5′-TCAAGGCTGAGAACGGGAAG-3′;

GAPDH-R: 5′-CTCCTCCTCCTCCTGCTTCT-3′.

Western Blot (WB) Analysis

Total cellular proteins were extracted using Radioimmunoprecipitation Assay (RIPA) lysis buffer supplemented with protease inhibitors (R0010, Solarbio, Beijing, China). Protein concentrations were measured, and 20 µg of each sample was separated on 10% Sodium Dodecyl Sulfate-Polyacrylamide Gel Electrophoresis (SDS-PAGE) gels before transfer to Polyvinylidene Fluoride (PVDF) membranes (10600023, Amersham, Freiburg, Germany). Membranes were blocked in 5% non-fat milk at room temperature for 1 h and incubated overnight at 4 °C with primary antibodies. After washing with Tris-Buffered Saline with Tween-20 (TBST), membranes were incubated with Horseradish Peroxidase (HRP)-conjugated secondary antibodies for 1 h at room temperature. Protein bands were

visualized using an Enhanced Chemiluminescence (34580, Thermo, Waltham, MA, USA) and quantified with ImageJ software (version 1.48b, NIH, Bethesda, MD, USA).

Primary antibodies included Claudin18.2 (700178, Invitrogen, Carlsbad, CA, USA; 1:100), ZO1 (617300, Thermo Fisher Scientific; 1:100), occludin (331500, Thermo Fisher Scientific; 1:100), Ecadherin (610181, BD Biosciences, San Jose, CA, USA; 1:200), and GAPDH (A19056, ABclonal, Wuhan, China; 1:200). HRP-conjugated goat anti-rabbit or goat anti-mouse secondary antibodies (PV6001/PV6002, Zhongshan Golden Bridge Biotechnology, Beijing, China; 1:200) were applied for 30 min at room temperature.

Immunofluorescence (IF) and Co-Localization Analysis

MKN45 cells were seeded on sterile glass coverslips in 6-well plates (2×10^5 cells per well) and cultured to approximately 70% confluence. Cells were fixed with 4% paraformaldehyde (P1110, Solarbio, Beijing, China) for 15 min at room temperature, rinsed three times with Phosphate-Buffered Saline (PBS), and permeabilized with 0.1% Triton X-100 (T8200, Solarbio, Beijing, China) for 10 min. After blocking with 5% bovine serum albumin (A8020, Solarbio, Beijing, China) for 1 h, cells were incubated overnight at 4 °C with primary antibodies against CLDN18.2 (700178, Invitrogen, Carlsbad, CA, USA; 1:100), ZO1 (617300, Thermo Fisher Scientific; 1:100), occludin (331500, Thermo Fisher Scientific; 1:100), or E-cadherin (610181, BD Biosciences, San Jose, CA, USA; 1:200).

Following three PBS washes, cells were incubated with Alexa Fluor 488- or Alexa Fluor 594-conjugated secondary antibodies (1:500; Invitrogen, Carlsbad, CA, USA; A-11008, A-11012) for 1 h at room temperature in the dark. Nuclei were counterstained with 4′,6-Diamidino-2-Phenylindole (DAPI) (1 µg/mL; C1002, Beyotime, Shanghai, China) for 5 min. Coverslips were mounted and imaged using a confocal laser scanning microscope (Leica TCS SP8, Leica Microsystems, Wetzlar, Germany). Imaging parameters were maintained constant for all samples.

siRNA-Mediated Knockdown of CLDN18.2

A specific small interfering RNA (siRNA) targeting CLDN18.2 was designed using an online siRNA design tool (http://sidirect2.rnai.jp/design.cgi) and synthesized by GeneChem (Shanghai, China). The sequences were: sense (guide) strand, 5′-ACAAAGACCUGAGACAAUGAA-3′; antisense (passenger) strand, 5′-CAUUGUCUCAGGUCUUUGUGC-3′. A non-targeting scrambled siRNA (5′-UUCUCCGAACGUGUCACGUTT-3′) served as the negative control. Cells were transfected with siRNAs at a final concentration of 50 nM using Lipofectamine™ RNAiMAX (13778075, Invitrogen, Carlsbad, CA, USA) following the manufacturer's instructions. After 48 h of transfection, cells were collected for downstream analyses.

FITC-Dextran Permeability Assay

MKN45 and SNU-16 cells were seeded onto Transwell inserts (0.4 µm pore size; 3413, Corning, Corning, NY, USA) and cultured until a continuous monolayer was established. Serum-free medium containing 1 mg/mL Fluorescein Isothiocyanate (FITC)-Dextran (FD4, Sigma-Aldrich, St. Louis, MO, USA) was added to the upper chamber, and an equal volume of PBS was added to the lower chamber. After 2 h of incubation, 100 µL of medium from the lower chamber was transferred to a black 96-well plate. Fluorescence intensity was measured using a microplate reader (BioTek Synergy H1, Vermont, USA) with an excitation wavelength of 485 nm and an emission wavelength of 528 nm. Permeability was calculated as:

$$\text{Permeability } (\%) = F_{\text{upper chamber}} / F_{\text{lower chamber}} \times 100\%.$$

All experiments were performed independently in triplicate.

Transepithelial Electrical Resistance (TEER) Measurement

MKN45 and SNU-16 cells were seeded onto Transwell inserts (0.4 µm pore size; 3413, Corning, Corning, NY, USA) and cultured until a confluent monolayer was established. To evaluate barrier integrity, serum-free medium containing 1 mg/mL FITC-Dextran (FD4, Sigma-Aldrich, St. Louis, MO, USA) was added to the apical chamber, while an equal volume of PBS was added to the basal compartment. Following a 2-hour incubation, 100 µL of medium from the lower chamber was collected into a black 96-well plate, and the fluorescence intensity was measured using a microplate reader (Synergy H1, BioTek, Vermont, USA) at an excitation wavelength of 485 nm and emission wavelength of 528 nm. Paracellular permeability was quantified using the following formula:

$$\text{TEER } (\Omega \cdot \text{cm}^2) = (R_{\text{sample}} - R_{\text{blank}}) \times A,$$

where A represents the membrane surface area (1.12 cm^2). All measurements were performed at 37 °C to ensure assay consistency and reproducibility.

Migration and Invasion Assays

Cell migratory capacity was evaluated using Transwell chambers with 8 µm pore-size polycarbonate membranes (3422, Corning, NY, USA). Transfected cells were resuspended in serum-free medium, and 1×10^5 cells were seeded into the upper chamber. The lower chamber was filled with medium containing 10% fetal bovine serum (PS-FB5-SA, Peak Inc., USA) as a chemoattractant. Chambers were incubated at 37 °C with 5% CO_2 for 24 h. For inva-

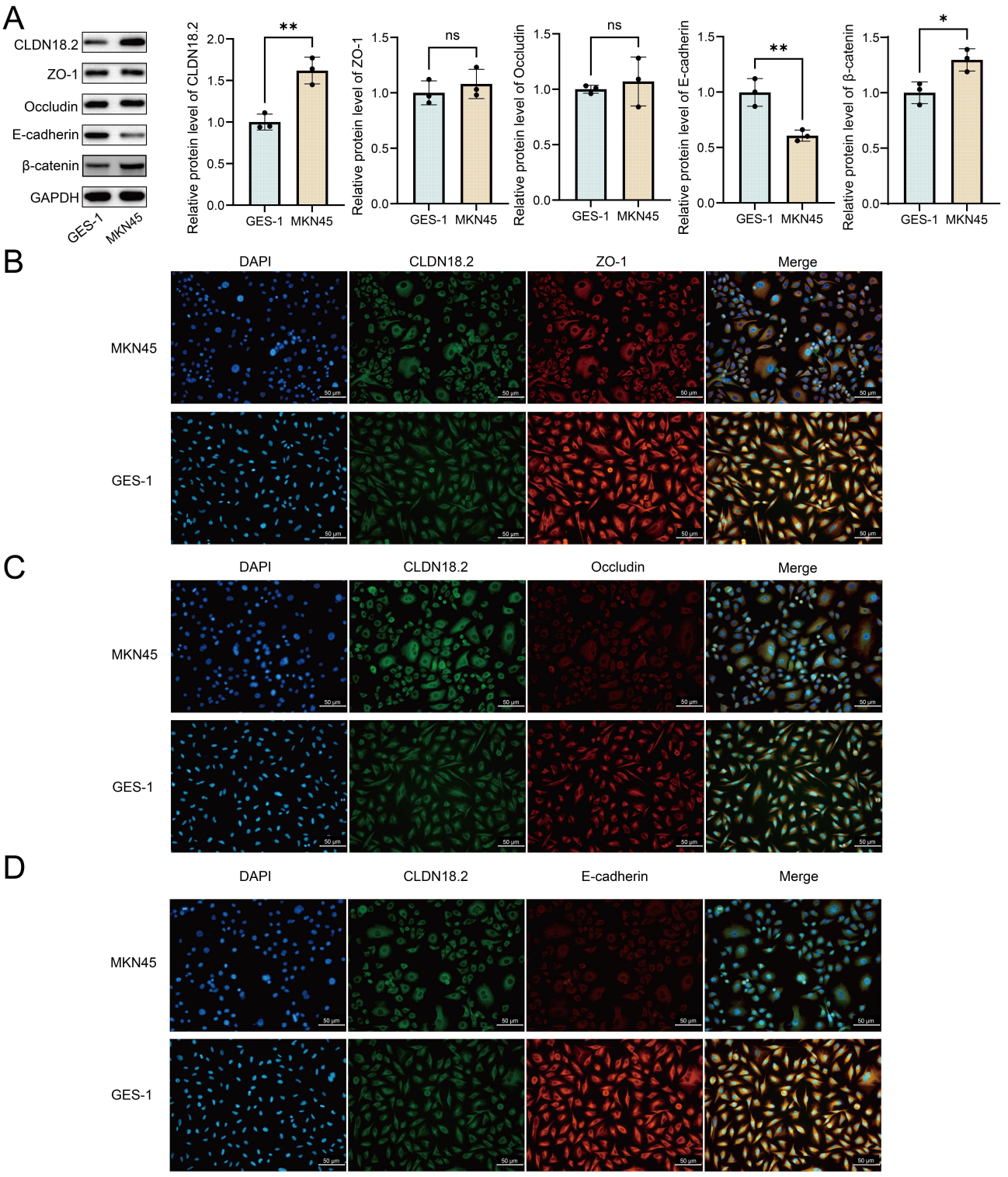

Fig. 1. Expression and subcellular localization of Claudin 18.2 (CLDN18.2) in gastric cancer and normal gastric epithelial cells. (A) Western blot analysis of CLDN18.2, ZO-1, E-cadherin, β-catenin, and occludin in MKN45 and GES-1 cells. (B) Immunofluorescence co-staining of CLDN18.2 (green) and Zonula occludens-1 (ZO-1) (red) in MKN45 and GES-1 cells. Nuclei were counterstained with 4′,6-Diamidino-2-Phenylindole (DAPI) (blue). Scale bar: 50 µm. (C) Immunofluorescence co-staining of CLDN18.2 (green) and occludin (red) in MKN45 and GES-1 cells. Scale bar: 50 µm. (D) Immunofluorescence co-staining of CLDN18.2 (green) and E-cadherin (red) in MKN45 and GES-1 cells. Scale bar: 50 µm. ns, not significant; *$p < 0.05$, **$p < 0.01$.

sion assays, the upper chamber membranes were pre-coated with Matrigel (1 mg/mL; 354234, Corning, NY, USA). After incubation, non-migrated or non-invaded cells on the upper membrane surface were removed. Cells adhering to the lower membrane were fixed with 4% paraformaldehyde (DF0135, Leagene Biotechnology, Beijing, China) for 15 min, stained with 0.1% crystal violet (C0775, Sigma-Aldrich, St. Louis, MO, USA) for 20 min, and then rinsed with PBS. Migrated or invaded cells were quantified by counting five randomly selected microscopic fields per membrane at 100× magnification.

Co-Immunoprecipitation (Co-IP) Assay

MKN45 cells were lysed on ice using RIPA buffer supplemented with protease inhibitors (R0010, Solarbio, Beijing, China). For each Co-IP reaction, 1 mg of total protein was incubated with 2 µg of anti-CLDN18.2 antibody (700178, Invitrogen, Carlsbad, CA, USA) or rabbit IgG (ab37415, Abcam, Cambridge, UK) as a negative control at 4 °C overnight under gentle rotation. Protein A/G magnetic beads (30 µL; 88802, Thermo Fisher Scientific, USA) were added and incubated for an additional 2 h at 4 °C. Beads were washed three times with lysis buffer to remove non-specifically bound proteins. Immunocomplexes were eluted with SDS sample buffer, separated by SDS-PAGE, and analyzed via Western blotting to detect ZO1 (617300, Thermo Fisher Scientific; 1:100). Ten percent of each lysate was reserved as an input control for comparison.

ZO-1 Overexpression (Rescue) Assay

The full-length human ZO-1 (TJP1) coding sequence (NCBI RefSeq: NM_003257.5, 5438 bp) was cloned into the pcDNA3.1(+) expression vector to generate the pcDNA3.1-ZO-1 plasmid (GeneChem, Shanghai, China). MKN45 cells were co-transfected with siCLDN18.2 and the ZO-1 overexpression construct using Lipofectamine™ 3000 (L3000015, Invitrogen) following the manufacturer's instructions (2 µg plasmid per well; 2×10^5 cells per well in 6-well plates). Cells transfected with the empty pcDNA3.1(+) vector (2 µg per well; GeneChem, Shanghai, China) served as the negative control.

Establishment of an Orthotopic Gastric Cancer Xenograft Model

Four-week-old male BALB/c nude mice (weighing 18–22 g) were obtained from Beijing Vital River Laboratory Animal Technology Co., Ltd. All animals were maintained under specific pathogen-free (SPF) conditions with controlled temperature (22 ± 2 °C), relative humidity (50–60%), and a 12-hour light/dark cycle. Sterilized chow and water were provided *ad libitum*, and experiments were initiated after a 7-day acclimation period.

The human gastric cancer cell line MKN45 (Cell Bank of the Chinese Academy of Sciences, Short Tandem Repeat-authenticated) was used to establish stably transfected cell lines with the following treatments: Control, siNC + OE-NC, siCLDN18.2 + OE-NC, siNC + OE-ZO-1, and siCLDN18.2 + OE-ZO-1. Stable clones were generated by lentiviral infection and selected with puromycin (2 µg/mL, Sigma-Aldrich, P8833) for 7 days. Mice were anesthetized with continuous inhalation of 2% isoflurane (RWD Life Science, model R510-22). Under sterile conditions, a midline abdominal incision (~1–1.5 cm) was made to expose the gastric body, and 50 µL of cell suspension (approximately 1×10^6 cells) was slowly injected into the subserosal layer of the stomach using a 30G needle. Following injection, the site was compressed with a sterile cotton swab for 30 s to prevent leakage, and both the peritoneum and skin were sutured.

Mice were placed on a 37 °C warming pad for post-operative recovery and monitored weekly for food intake and general activity. Euthanasia was performed using a gradual-fill CO_2 method, introducing CO_2 at 20–30% of chamber volume per minute until respiratory arrest, followed by cervical dislocation to confirm death before tissue collection. The abdomen was opened immediately to collect tissue samples and examine pulmonary metastatic nodules.

All animal procedures adhered to institutional guidelines for laboratory animal care. The study protocol was reviewed and approved by the Animal Ethics Committee of Xuzhou Hejia Hospital (Approval No. hpfc-1-2022-01).

Statistical Analysis

All statistical analyses were performed using GraphPad Prism 9.0 (GraphPad Software, San Diego, CA, USA). The normality of datasets was evaluated using the Shapiro–Wilk test. For comparisons between two groups, normally distributed variables were analyzed using Student's *t*-test, whereas non-normally distributed variables were evaluated with the Mann–Whitney U test. For comparisons across multiple groups, One-Way Analysis of Variance (ANOVA) or the Kruskal–Wallis test was applied, followed by Tukey's post hoc test. Paired data were analyzed using either the paired *t*-test or the Wilcoxon signed-rank test, as appropriate. Data are expressed as mean ± standard deviation (SD), and statistical significance was defined as $p < 0.05$.

Results

Expression and Subcellular Localization of CLDN18.2

Western blot analysis demonstrated that CLDN18.2 expression was markedly elevated in the gastric cancer cell line MKN45 compared with normal gastric epithelial cells (GES-1). Correspondingly, E-cadherin protein levels were significantly reduced in MKN45 cells ($p < 0.01$), while β-catenin exhibited a modest increase ($p < 0.05$). No significant differences in ZO-1 or occludin expression were observed between the two cell lines ($p > 0.05$) (Fig. 1A).

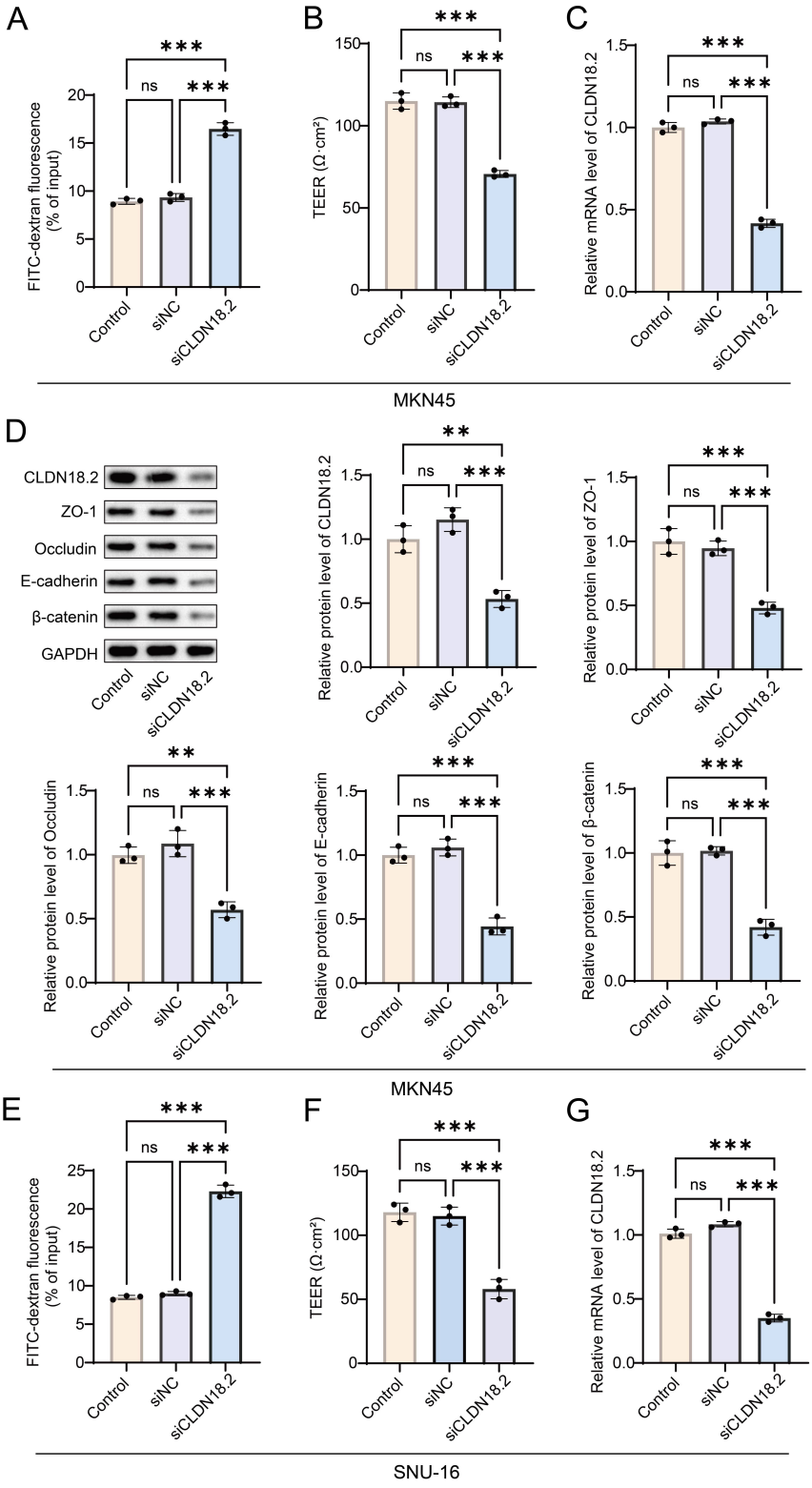

Fig. 2. Functional effects of CLDN18.2 knockdown on epithelial barrier integrity and junctional protein expression in MKN45 cells. (A) Fluorescein Isothiocyanate (FITC)-Dextran permeability assay in the MKN45 cell line. (B) Transepithelial electrical resistance (TEER) measurements in the MKN45 cell line. (C) Quantitative Real-Time Polymerase Chain Reaction (qPCR) analysis confirming CLDN18.2 knockdown efficiency in the MKN45 cell line. (D) Western blot analysis of CLDN18.2, ZO-1, occludin, E-cadherin, and β-catenin in the MKN45 cell line. (E) FITC-Dextran permeability assay in the SNU-16 cell line. (F) TEER measurement in the SNU-16 cell line. (G) qPCR analysis confirming CLDN18.2 knockdown efficiency in the SNU-16 cell line. ns, not significant; $^{**}p < 0.01$, $^{***}p < 0.001$.

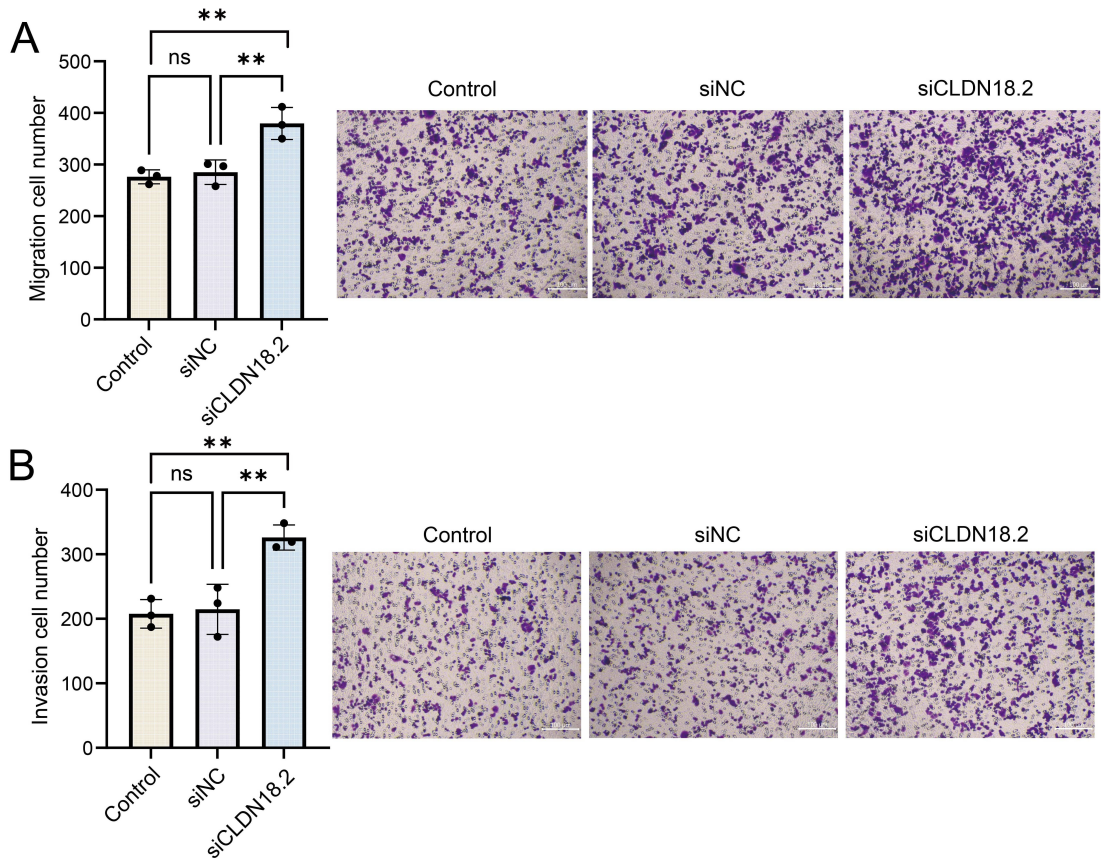

Fig. 3. CLDN18.2 knockdown enhances migratory and invasive behaviors of MKN45 cells. (A) Transwell migration assay. (B) Transwell invasion assay. Scale bar: 100 µm. ns, not significant; $^{**}p < 0.01$.

Immunofluorescence co-localization analysis revealed that in both MKN45 and GES-1 cells, CLDN18.2 (green) exhibited spatial overlap with ZO-1, occludin, and E-cadherin (red) at the cell membrane (Fig. 1B–D). Collectively, these findings indicate that CLDN18.2 is primarily localized at the plasma membrane in MKN45 cells and co-localizes with the tight junction components ZO-1 and occludin, suggesting a potential role in regulating or remodeling intercellular junctional architecture in gastric cancer.

Effect of CLDN18.2 Knockdown on Tight Junction Integrity and Epithelial Barrier Function

To further evaluate the contribution of CLDN18.2 to epithelial barrier integrity, CLDN18.2 expression was silenced in MKN45 and SNU-16 gastric cancer cells. FITC-Dextran permeability assays revealed a significant increase in paracellular flux following CLDN18.2 knockdown compared with both the untreated control and siNC groups ($p < 0.001$), whereas no differences were observed between control and siNC cells ($p > 0.05$) (Fig. 2A). Consistently, transepithelial electrical resistance (TEER) measurements demonstrated a marked reduction in epithelial barrier strength in siCLDN18.2 cells compared with controls ($p < 0.001$), with no significant difference between the blank and siNC groups ($p > 0.05$) (Fig. 2B). qPCR analysis confirmed efficient CLDN18.2 depletion, with relative mRNA expression decreasing from 1.12 ± 0.03 in siNC cells to 0.25 ± 0.03 in siCLDN18.2 cells ($p < 0.001$) (Fig. 2C).

At the protein level, Western blotting demonstrated a substantial reduction in CLDN18.2 following knockdown ($p < 0.001$), accompanied by pronounced decreases in the tight junction proteins ZO-1 and occludin (both $p < 0.001$) and in the adherens junction proteins E-cadherin and β-catenin (both $p < 0.001$). No statistically significant differences were observed between the blank and siNC groups ($p > 0.05$) (Fig. 2D). Parallel validation in SNU-16 cells yielded consistent outcomes, with silencing of CLDN18.2 significantly increasing paracellular permeability, reducing TEER ($p < 0.001$), and markedly lowering CLDN18.2 mRNA levels ($p < 0.001$) (Fig. 2E–G). Collectively, these findings indicate that CLDN18.2 depletion disrupts tight junction architecture, compromises epithelial barrier function, and facilitates increased paracellular permeability in gastric cancer cells.

Effect of CLDN18.2 Knockdown on Junctional Protein Expression and Cell Invasion/Migration

Transwell assays revealed that silencing CLDN18.2 markedly increased both the invasive ($p < 0.01$) and mi-

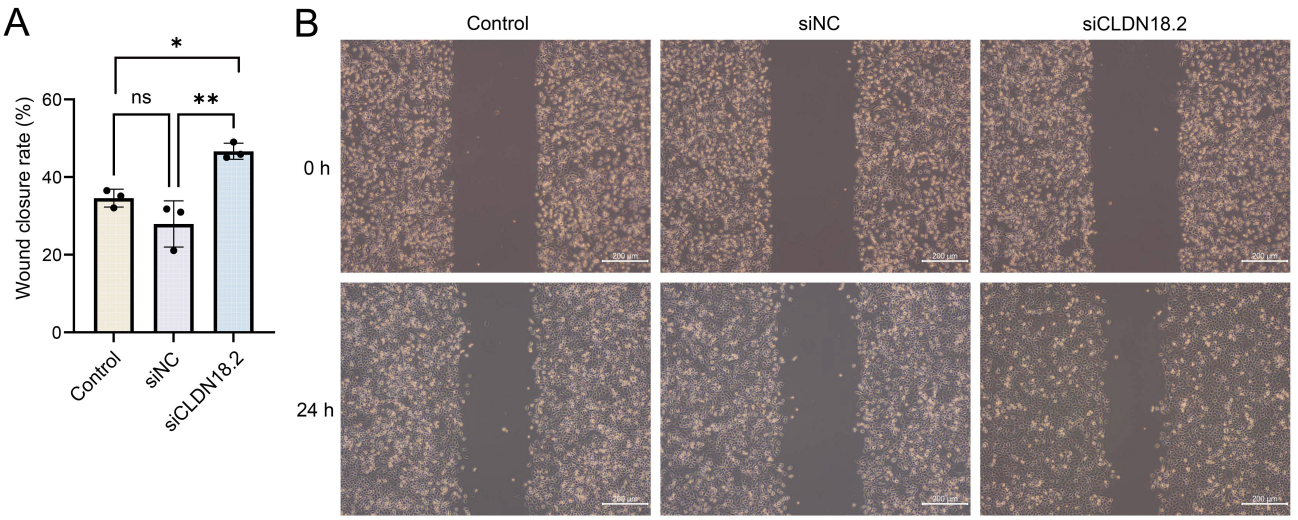

Fig. 4. Wound healing assay demonstrates enhanced migratory capacity following CLDN18.2 knockdown. (A) Quantification of wound closure rate. (B) Representative images of scratch wounds at 0 h and 24 h. Scale bar: 200 µm. ns, not significant; *$p < 0.05$, **$p < 0.01$.

gratory ($p < 0.01$) capabilities of MKN45 cells, whereas no significant differences were observed between the blank and siNC control groups ($p > 0.05$) (Fig. 3A,B). Consistently, wound healing assays demonstrated that CLDN18.2 knockdown significantly accelerated cell migration, reflected by a higher wound closure rate compared with siNC cells ($p < 0.01$) (Fig. 4A,B). Together, these findings indicate that downregulation of CLDN18.2 reduces the expression of key junctional proteins, including ZO-1, occludin, E-cadherin, and β-catenin, thereby weakening intercellular junction integrity and substantially enhancing the migratory and invasive behavior of gastric cancer cells.

Molecular Interaction Between CLDN18.2 and ZO-1

Pull-down assays using an anti-CLDN18.2 antibody demonstrated that CLDN18.2 specifically co-immunoprecipitated ZO-1 in MKN45 cells, whereas only a minimal background band was observed in the IgG negative control, confirming the specificity of the CLDN18.2–ZO-1 interaction (Fig. 5A). The input samples (10%) showed clear ZO-1 bands. Notably, following siCLDN18.2 treatment, the co-precipitation of ZO-1 was markedly reduced. These findings indicate that CLDN18.2 interacts with ZO-1 within a protein complex, and this interaction is dependent on the expression levels of CLDN18.2.

Rescue Experiment: ZO-1 Overexpression Restores Tight Junction Integrity Following CLDN18.2 Silencing

In MKN45 cells, qPCR analysis confirmed the efficiency of CLDN18.2 knockdown and ZO-1 overexpression at the mRNA level ($p < 0.001$) (Fig. 5B). CLDN18.2 silencing significantly decreased protein levels of ZO-1, occludin, E-cadherin, and β-catenin ($p < 0.01$). Upon ZO-1 overexpression (siCLDN18.2 + OE-ZO-1 group), ZO-1 protein expression increased from 0.6 ± 0.06 to 1.85 ± 0.10 ($p < 0.001$), occludin from 0.53 ± 0.04 to 1.39 ± 0.06 ($p < 0.001$), E-cadherin from 0.59 ± 0.11 to 1.52 ± 0.21 ($p < 0.001$), and β-catenin from 0.39 ± 0.04 to 0.97 ± 0.07 ($p < 0.001$), whereas CLDN18.2 levels remained unchanged ($p > 0.05$) (Fig. 5C).

FITC-Dextran permeability assays demonstrated that CLDN18.2 knockdown significantly increased paracellular permeability ($p < 0.001$). ZO-1 overexpression partially reduced permeability to $19.83\% \pm 1.23\%$ ($p < 0.001$), indicating partial restoration of epithelial barrier function (Fig. 5D). Similarly, TEER measurements revealed that CLDN18.2 silencing reduced resistance from 385.3 ± 17.8 $\Omega \cdot cm^2$ to 148.7 ± 9.1 $\Omega \cdot cm^2$ ($p < 0.001$), while ZO-1 overexpression restored TEER to 252.0 ± 14.0 $\Omega \cdot cm^2$ ($p < 0.001$), demonstrating partial recovery of tight junction integrity (Fig. 5E). These findings collectively indicate that ZO-1 overexpression can partially rescue the downregulation of tight junction proteins and the barrier dysfunction induced by CLDN18.2 depletion.

In Vivo Validation of the CLDN18.2–ZO-1 Regulatory Axis in Gastric Cancer Metastasis

To further validate the *in vitro* findings, an orthotopic xenograft mouse model was established using MKN45 cells with stable knockdown of CLDN18.2 and/or overexpression of ZO-1. The number of metastatic nodules was markedly increased in the siCLDN18.2 + OE-NC group compared with the control and siNC + OE-NC groups ($p < 0.001$). In contrast, ZO-1 overexpression (siCLDN18.2 + OE-ZO-1) partially reversed this pro-metastatic effect, resulting in a significant reduction in metastatic nodules

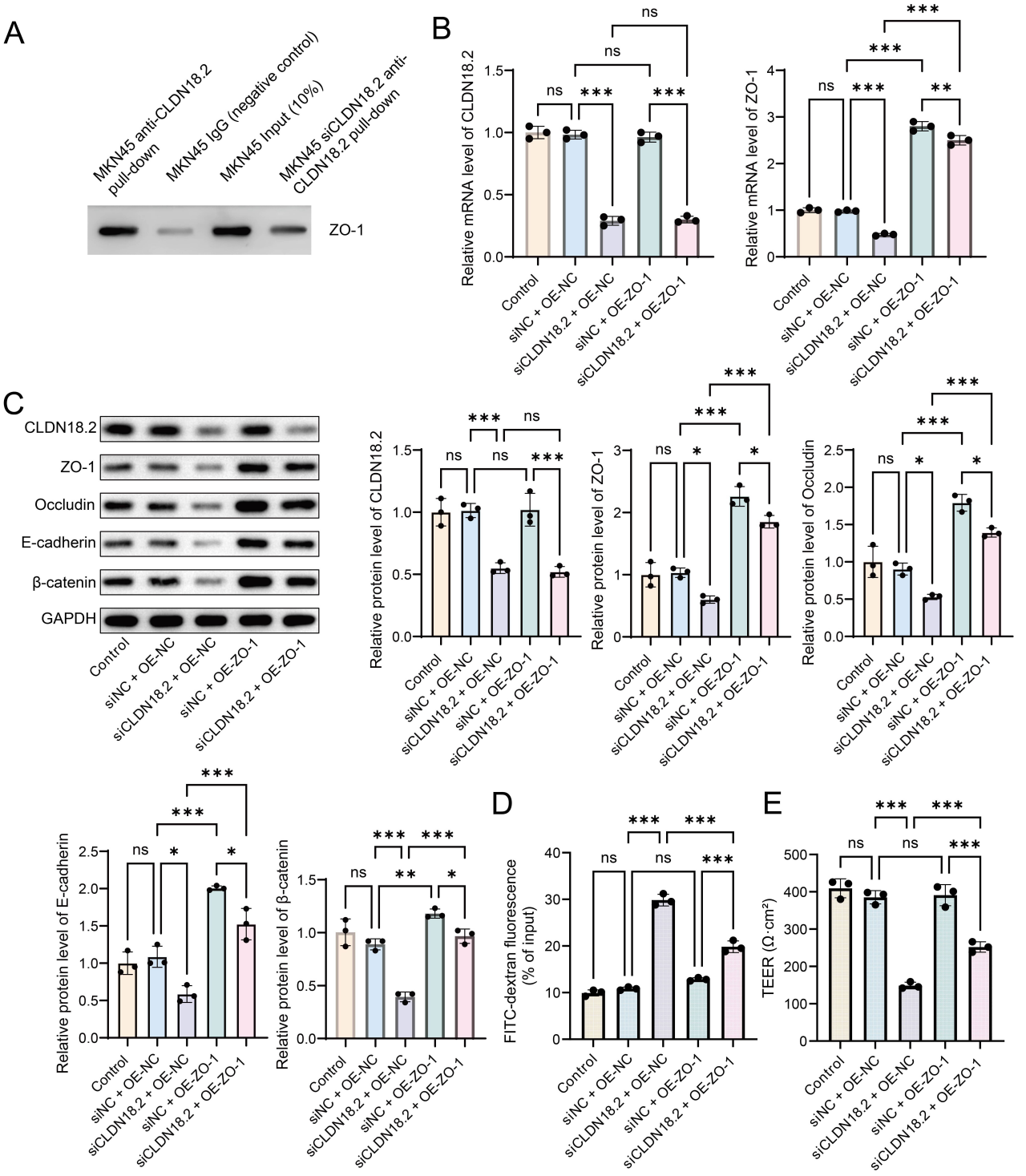

Fig. 5. CLDN18.2 interacts with ZO-1, and ZO-1 overexpression partially restores tight junction protein expression and barrier integrity. (A) Co-immunoprecipitation showing reduced ZO-1 co-precipitation upon CLDN18.2 knockdown. Input represents 10% of the total lysate; IgG serves as a negative control. (B) qPCR analysis of CLDN18.2 and ZO-1 mRNA expression. (C) Western blot analysis of junctional protein expression. (D) FITC-Dextran permeability assay. (E) TEER measurement. ns, not significant; *$p < 0.05$, **$p < 0.01$, ***$p < 0.001$.

($p < 0.001$). Overexpression of ZO-1 alone (siNC + OE-ZO-1) did not promote metastasis and showed a comparable or slightly lower metastatic burden relative to controls (Fig. 6A).

qPCR analysis confirmed that CLDN18.2 expression was markedly reduced in the siCLDN18.2 + OE-NC group and remained low in the siCLDN18.2 + OE-ZO-1 group ($p < 0.001$). Overexpression of ZO-1 markedly increased ZO-

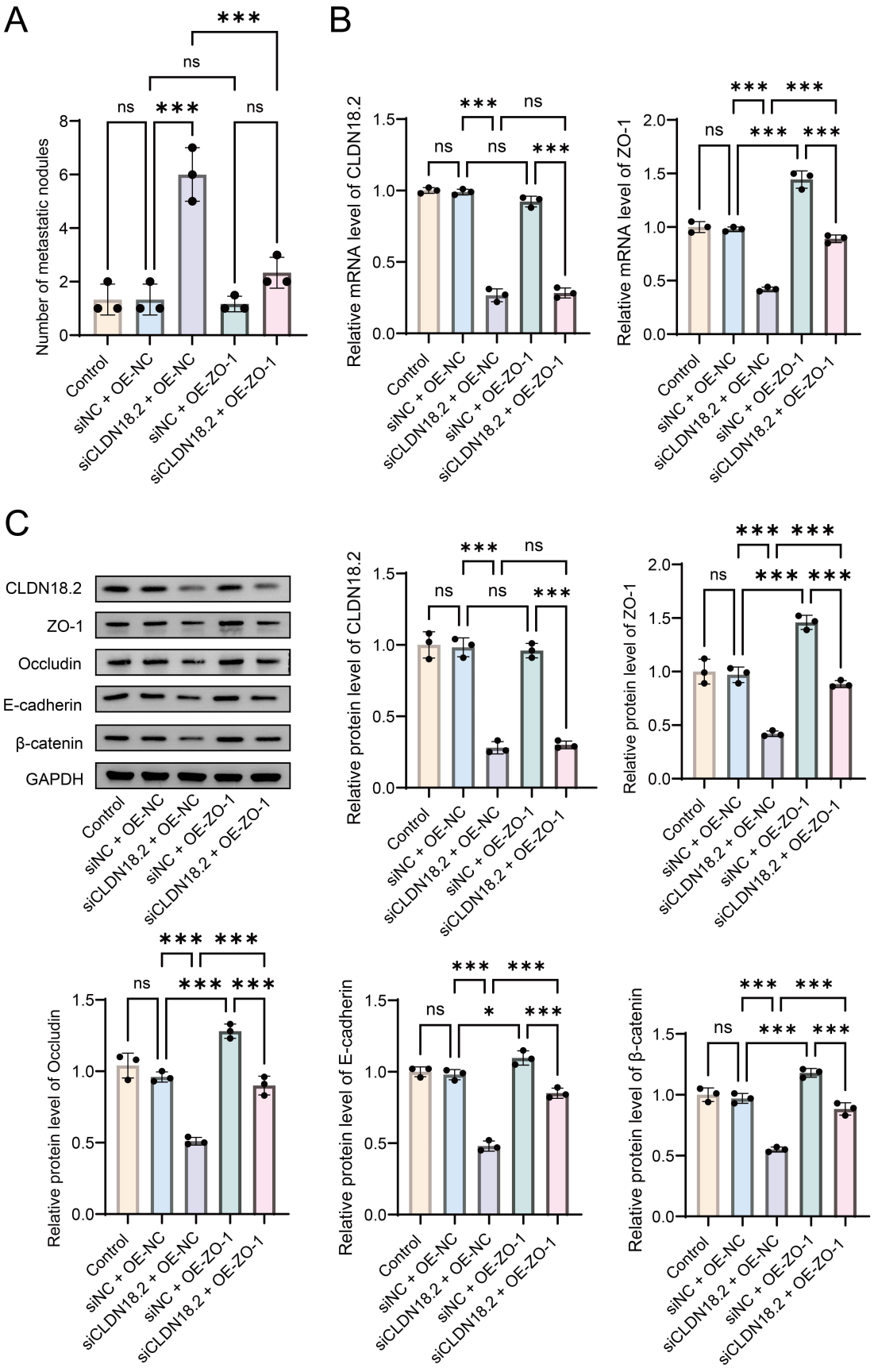

Fig. 6. ***In vivo*** **validation of the CLDN18.2–ZO-1 axis in gastric cancer metastasis.** (A) Quantification of metastatic nodules across experimental groups. (B) qPCR analysis of CLDN18.2 and ZO-1 mRNA expression. (C) Western blot analysis of CLDN18.2, ZO-1, occludin, E-cadherin, and β-catenin in xenograft tumor tissues. ns, not significant; *$p < 0.05$, ***$p < 0.001$.

1 mRNA in the siNC + OE-ZO-1 group ($p < 0.001$). ZO-1 expression in the siCLDN18.2 + OE-ZO-1 group returned to a level comparable to the control group and was significantly higher than that in the siCLDN18.2 + OE-NC group ($p < 0.001$) (Fig. 6B).

Western blot analysis of tumor tissues revealed that CLDN18.2 knockdown resulted in a pronounced downregulation of ZO-1, occludin, E-cadherin, and β-catenin (all $p < 0.001$), consistent with the disruption of tight and adherens junctions. Overexpression of ZO-1 significantly restored the expression of these junctional proteins ($p < 0.001$), whereas CLDN18.2 protein remained unchanged, confirming that ZO-1 acts downstream of CLDN18.2 to maintain epithelial integrity and suppress tumor progression (Fig. 6C).

Discussion

CLDN18.2 is a TJ protein specifically expressed in gastric mucosal epithelium and has gained attention as a potential therapeutic target in gastric cancer [8]. In this study, we systematically investigated its role in maintaining TJ integrity and suppressing the migratory and invasive behavior of gastric cancer cells. We observed that CLDN18.2 localized to the plasma membrane of MKN45 cells and co-localized with the TJ scaffold protein ZO-1. Silencing CLDN18.2 resulted in significant downregulation of ZO-1, occludin, E-cadherin, and β-catenin, along with increased FITC-Dextran permeability and decreased TEER, ultimately enhancing cell migration and invasion. Although ZO-1 overexpression partially reversed the downregulation of TJ proteins and improved barrier dysfunction, it did not restore CLDN18.2 expression. These findings support CLDN18.2 as a key regulator of epithelial barrier integrity and a suppressor of cancer cell motility, highlighting the functional significance of the CLDN18.2–ZO-1 regulatory axis in gastric cancer progression.

CLDN18.2 is essential for preserving epithelial barrier integrity in gastric cancer cells. Silencing CLDN18.2 significantly increased paracellular permeability, as demonstrated by FITC-Dextran assays, and markedly reduced TEER, indicating compromised intercellular junction strength. Tight junction proteins, including the Claudin family, occludin, and ZO-1, are essential components of epithelial barrier function, and their loss is frequently associated with barrier disruption and elevated epithelial permeability [17]. Cao *et al.* [6] reported that CLDN18.2 in normal gastric epithelium prevents H^+ leakage, thereby maintaining mucosal homeostasis. Our findings extend this principle to gastric cancer cells, demonstrating that reduced CLDN18.2 expression compromises both molecular selectivity and ion-barrier properties of the epithelial layer.

We further observed that CLDN18.2 knockdown induced a simultaneous reduction in multiple junctional proteins, which corresponded with significantly enhanced migration and invasion. Notably, the TJ proteins ZO-1 and occludin, as well as the adherens junction components E-cadherin and β-catenin, were markedly reduced. Consistently, transwell and wound healing assays demonstrated increased motility and invasiveness of MKN45 cells. These observations align with features of EMT during tumorigenesis. Loss of E-cadherin is a well-established mechanism that reduces cell-cell adhesion, promoting detachment and acquisition of migratory and invasive capacities [18]. Moreover, loss of tight junction proteins is commonly observed in high-grade malignancies. In poorly differentiated gastric cancers, both occludin and ZO-1 are markedly reduced and correlate with increased invasive potential [19]. Consistent with these reports, our findings indicate that CLDN18.2 downregulation destabilizes tight and adherens junctions, reduces E-cadherin/β-catenin expression, compromises intercellular adhesion, and consequently enhances the migration and invasion of gastric cancer cells.

Clinical studies support a strong association between reduced CLDN18.2 expression and tumor metastasis. Kim *et al.* [11] observed significantly lower levels of CLDN18.2 and E-cadherin in peritoneal metastases compared with non-metastatic tissues, with a positive correlation between these two markers. Similarly, analyses of resected gastric cancer cohorts have demonstrated that CLDN18.2-positive tumors tend to exhibit shallower invasion and lower rates of lymphovascular infiltration [20]. Collectively, these findings indicate that CLDN18.2 may function as a metastasis suppressor in gastric cancer, and that its downregulation could facilitate the acquisition of invasive phenotypes.

We observed through co-immunoprecipitation that CLDN18.2 forms a complex with ZO-1, and this interaction was markedly attenuated following CLDN18.2 downregulation. The C-terminal tail of Claudin family proteins contains a Postsynaptic Density protein 95/Discs Large/Zona Occludens-1 (PDZ)-binding motif capable of interacting with the PDZ domains of TJ scaffold proteins such as ZO-1, thereby linking membrane-localized Claudins and occludin to the actin cytoskeleton [21]. Our findings provide the first direct evidence that CLDN18.2 specifically binds ZO-1, suggesting that CLDN18.2 contributes to the assembly or stabilization of tight junction complexes in gastric cancer cells. Previous animal studies have further shown that knockout of Claudin-18 family members disrupts epithelial barrier function and promotes gastric tumorigenesis [22], highlighting the essential role of Claudin–ZO-1 structures in maintaining epithelial homeostasis [23].

Further, ZO-1 overexpression experiments confirmed the pivotal role of ZO-1 in CLDN18.2-mediated tight junction regulation. Restoration of ZO-1 expression partially reversed the reductions in occludin and E-cadherin induced by CLDN18.2 loss, decreased paracellular permeability, and elevated TEER, indicating partial recovery of barrier function. These findings are consistent with previous reports, which show that ZO-1, as a central scaffold

protein, stabilizes tight junction architecture and restricts paracellular permeability [24]. Collectively, these findings demonstrate that ZO-1 overexpression can compensate for the loss of junctional proteins and barrier integrity caused by CLDN18.2 deficiency, supporting the principle that CLDN18.2 function depends on ZO-1-mediated structural stabilization.

This study highlights CLDN18.2 as a pivotal determinant of epithelial integrity and metastatic potential in gastric cancer through its regulation of ZO-1 and tight junction stability. The finding that ZO-1 overexpression can partially rescue CLDN18.2 loss-induced barrier disruption underscores a potentially targetable CLDN18.2–ZO-1 regulatory axis. Given the emerging success of CLDN18.2-targeted therapies, including zolbetuximab and bispecific antibodies, our findings provide mechanistic evidence supporting their clinical rationale, not only by identifying tumor-specific epitopes but also by linking CLDN18.2 deficiency to enhanced invasiveness. These insights suggest that restoring tight junction integrity or enhancing ZO-1 function could represent promising adjunct therapeutic strategies for CLDN18.2-low or treatment-resistant tumors.

However, several limitations should be acknowledged. This study was conducted primarily using a single gastric cancer cell line and an orthotopic xenograft model, which may not fully reflect the heterogeneity of human gastric cancer. Moreover, the precise upstream regulators and downstream signaling cascades linking CLDN18.2–ZO-1 interactions to EMT remain to be elucidated. Future investigations integrating multi-omics profiling and patient-derived organoid models are warranted to validate these findings and explore combinatorial therapeutic strategies that target both junctional integrity and immune responsiveness.

Conclusion

In summary, CLDN18.2 preserves epithelial barrier function and suppresses gastric cancer progression by stabilizing ZO-1-mediated tight junctions. Loss of CLDN18.2 compromises junctional integrity, enhances invasiveness, and promotes metastasis, whereas compensatory restoration of ZO-1 mitigates these effects. These findings not only deepen the mechanistic understanding of CLDN18.2 in tumor biology but also provide a translational framework for optimizing CLDN18.2-targeted therapies and developing novel strategies to enhance epithelial cohesion in aggressive gastric cancers.

Availability of Data and Materials

The experimental data used to support the findings of this study are available from the corresponding author upon request.

Author Contributions

WL performed the majority of the experiments, analyzed the data, and contributed to the writing and revision of the manuscript. MC contributed to data acquisition and manuscript drafting. BQ interpreted the results and critically revised the manuscript. XL conceived and supervised the project, critically revised the manuscript for important intellectual content, and provided final approval of the manuscript. All authors have read and approved the final version of the manuscript and agreed to be accountable for all aspects of the work.

Ethics Approval and Consent to Participate

The study protocol was reviewed and approved by the Animal Ethics Committee of Xuzhou Hejia Hospital (Approval No. hpfc-1-2022-01).

Acknowledgment

Not applicable.

Funding

This research received no external funding.

Conflict of Interest

The authors declare no conflict of interest.

References

[1] Bray F, Laversanne M, Sung H, Ferlay J, Siegel RL, Soerjomataram I, *et al*. Global cancer statistics 2022: GLOBOCAN estimates of incidence and mortality worldwide for 36 cancers in 185 countries. CA: A Cancer Journal for Clinicians. 2024; 74: 229–263. https://doi.org/10.3322/caac.21834.

[2] Varga Z, Bíró A, Török M, Tóth D. A combined approach for individualized lymphadenectomy in gastric cancer patients. Pathology and Oncology Research. 2023; 29: 1611270. https://doi.org/10.3389/pore.2023.1611270.

[3] Mathias-Machado MC, de Jesus VHF, Jácome A, Donadio MD, Aruquipa MPS, Fogacci J, *et al*. Claudin 18.2 as a New Biomarker in Gastric Cancer-What Should We Know? Cancers. 2024; 16: 679. https://doi.org/10.3390/cancers16030679.

[4] Kalin M, Duzgun O. Long-term results of conversion surgery for advanced gastric cancer. Annali Italiani di Chirurgia. 2023; 94: 454–459.

[5] Kyuno D, Takasawa A, Kikuchi S, Takemasa I, Osanai M, Kojima T. Role of tight junctions in the epithelial-to-mesenchymal transition of cancer cells. Biochimica et Biophysica Acta. Biomembranes. 2021; 1863: 183503. https://doi.org/10.1016/j.bbamem.2020.183503.

[6] Cao W, Xing H, Li Y, Tian W, Song Y, Jiang Z, *et al*. Claudin18.2 is a novel molecular biomarker for tumor-targeted immunotherapy. Biomarker Research. 2022; 10: 38. https://doi.org/10.1186/s40364-022-00385-1.

[7] Kyuno D, Takasawa A, Takasawa K, Ono Y, Aoyama T, Magara K, *et al*. Claudin-18.2 as a therapeutic target in cancers: cumulative findings from basic research and clinical trials. Tissue

Barriers. 2022; 10: 1967080. https://doi.org/10.1080/21688370.2021.1967080.

[8] Coati I, Lotz G, Fanelli GN, Brignola S, Lanza C, Cappellesso R, *et al*. Claudin-18 expression in oesophagogastric adenocarcinomas: a tissue microarray study of 523 molecularly profiled cases. British Journal of Cancer. 2019; 121: 257–263. https://doi.org/10.1038/s41416-019-0508-4.

[9] Arnold A, Daum S, von Winterfeld M, Berg E, Hummel M, Rau B, *et al*. Prognostic impact of Claudin 18.2 in gastric and esophageal adenocarcinomas. Clinical & Translational Oncology. 2020; 22: 2357–2363. https://doi.org/10.1007/s12094-020-02380-0.

[10] Rohde C, Yamaguchi R, Mukhina S, Sahin U, Itoh K, Türeci Ö. Comparison of Claudin 18.2 expression in primary tumors and lymph node metastases in Japanese patients with gastric adenocarcinoma. Japanese Journal of Clinical Oncology. 2019; 49: 870–876. https://doi.org/10.1093/jjco/hyz068.

[11] Kim SR, Shin K, Park JM, Lee HH, Song KY, Lee SH, *et al*. Clinical Significance of CLDN18.2 Expression in Metastatic Diffuse-Type Gastric Cancer. Journal of Gastric Cancer. 2020; 20: 408–420. https://doi.org/10.5230/jgc.2020.20.e33.

[12] Itoh M, Nagafuchi A, Moroi S, Tsukita S. Involvement of ZO-1 in cadherin-based cell adhesion through its direct binding to alpha catenin and actin filaments. The Journal of Cell Biology. 1997; 138: 181–192. https://doi.org/10.1083/jcb.138.1.181.

[13] Al-Sadi R, Khatib K, Guo S, Ye D, Youssef M, Ma T. Occludin regulates macromolecule flux across the intestinal epithelial tight junction barrier. American Journal of Physiology. Gastrointestinal and Liver Physiology. 2011; 300: G1054–64. https://doi.org/10.1152/ajpgi.00055.2011.

[14] Bazellières E, Conte V, Elosegui-Artola A, Serra-Picamal X, Bintanel-Morcillo M, Roca-Cusachs P, *et al*. Control of cell-cell forces and collective cell dynamics by the intercellular adhesome. Nature Cell Biology. 2015; 17: 409–420. https://doi.org/10.1038/ncb3135.

[15] Dumortier JG, Martin S, Meyer D, Rosa FM, David NB. Collective mesendoderm migration relies on an intrinsic directionality signal transmitted through cell contacts. Proceedings of the National Academy of Sciences of the United States of America. 2012; 109: 16945–16950. https://doi.org/10.1073/pnas.1205870109.

[16] Cheng Y, Wen M, Wang X, Zhu H. Oncogene 5'-3' exoribonuclease 2 enhances epidermal growth factor receptor signaling pathway to promote epithelial-mesenchymal transition and metastasis in non-small-cell lung cancer. CytoJournal. 2024; 21: 46. https://doi.org/10.25259/Cytojournal_49_2024.

[17] Ohtani S, Terashima M, Satoh J, Soeta N, Saze Z, Kashimura S, *et al*. Expression of tight-junction-associated proteins in human gastric cancer: downregulation of claudin-4 correlates with tumor aggressiveness and survival. Gastric Cancer. 2009; 12: 43–51. https://doi.org/10.1007/s10120-008-0497-0.

[18] Zhao H, Hu H, Chen B, Xu W, Zhao J, Huang C, *et al*. Overview on the Role of E-Cadherin in Gastric Cancer: Dysregulation and Clinical Implications. Frontiers in Molecular Biosciences. 2021; 8: 689139. https://doi.org/10.3389/fmolb.2021.689139.

[19] Martin TA, Jiang WG. Loss of tight junction barrier function and its role in cancer metastasis. Biochimica et Biophysica Acta. 2009; 1788: 872–891. https://doi.org/10.1016/j.bbamem.2008.11.005.

[20] Kim HD, Choi E, Shin J, Lee IS, Ko CS, Ryu MH, *et al*. Clinicopathologic features and prognostic value of claudin 18.2 overexpression in patients with resectable gastric cancer. Scientific Reports. 2023; 13: 20047. https://doi.org/10.1038/s41598-023-47178-6.

[21] Tsukita S, Tanaka H, Tamura A. The Claudins: From Tight Junctions to Biological Systems. Trends in Biochemical Sciences. 2019; 44: 141–152. https://doi.org/10.1016/j.tibs.2018.09.008.

[22] Hagen SJ, Ang LH, Zheng Y, Karahan SN, Wu J, Wang YE, *et al*. Loss of Tight Junction Protein Claudin 18 Promotes Progressive Neoplasia Development in Mouse Stomach. Gastroenterology. 2018; 155: 1852–1867. https://doi.org/10.1053/j.gastro.2018.08.041.

[23] Dithmer S, Blasig IE, Fraser PA, Qin Z, Haseloff RF. The Basic Requirement of Tight Junction Proteins in Blood-Brain Barrier Function and Their Role in Pathologies. International Journal of Molecular Sciences. 2024; 25: 5601. https://doi.org/10.3390/ijms25115601.

[24] Van Itallie CM, Fanning AS, Bridges A, Anderson JM. ZO-1 stabilizes the tight junction solute barrier through coupling to the perijunctional cytoskeleton. Molecular Biology of the Cell. 2009; 20: 3930–3940. https://doi.org/10.1091/mbc.e09-04-0320.